

Fabrication and Characteristics of Fully-transparent Al-Sn-Zn-O TFTs Fabricated on glass at Low Temperature

Yingying Cong¹, Dedong Han^{1*}, Jing Wu^{1,2}, Nanan Zhao^{1,2}, Zhuofa Chen^{1,2}, Feilong Zhao^{1,2}, Junchen Dong^{1,2}, Shengdong Zhang², Xing Zhang¹ and Yi Wang^{1*}

¹Institute of Microelectronics, Peking University, Beijing 100871, China

²Shenzhen Graduate School, Peking University, Shenzhen 518055, China

Phone:+86-10-62766516 Fax:+86-10-62751789 *E-mail: handedong@pku.edu.cn, wangyi@ime.pku.edu.cn

Abstract

Fully-transparent Al-Sn-Zn-O thin film transistors (ATZO TFTs) with excellent electrical performance have been successfully fabricated on glass at low temperature. The I_{on}/I_{off} , μ_{FE} and V_T of the ATZO TFT are 1.18×10^7 , $102.38 \text{ cm}^2/\text{Vs}$, 1.62 V , respectively. Furthermore, the characteristics of ATZO TFTs with different compositions are compared and analyzed.

1. Introduction

Due to the excellent performance of high mobility, transparency and low temperature process, transparent oxide semiconductor thin film transistors have been investigated intensely for their promising applications in AMOLED and other advanced display technologies. So far, various novel oxide semiconductors for the active channel have been explored, such as In-Ga-Zn-O (IGZO) [1], Al-Zn-O (AZO) [2], Al-Sn-Zn-In-O [3] and so on. It is reported that In and Sn elements can enhance the carrier mobility [4], Al and Ga dopants strengthen the stability and suppress oxygen vacancies [5, 6]. However, Ga and In elements are both toxic and rare metals, which are unsuitable for sustainable mass production. So our researches focus on the Al-Sn-Zn-O (ATZO) material, which is much cheaper and remarkable performance material [7]. In addition, the composition of multielement oxide has an influence on the properties of TFTs. The Al and Sn elements can promote the electrical characteristics, but excess addition can distort the crystal structure and decrease the mobility. So the compromise between them is worth investigating.

In this paper, we compare the characteristics of ATZO TFTs with two kinds of appropriate compositions, and finally fabricate the two excellent ATZO TFTs, which demonstrate respective competitive advantages.

2. Experiment

During this fabrication process, 3-mask photolithography and standard lift-off technique were adopted. The ATZO TFTs were conventional bottom-gate top-contact structure, which were shown in Fig. 1. The width-to-length ratio was $100 \mu\text{m}/5 \mu\text{m}$. First, an Indium Tin Oxide (ITO) gate electrode, which was 130-nm-thick, was deposited on the glass substrate by RF magnetron sputtering. Second, a 150-nm-thick SiO_2 insulator was grown by plasma-enhanced chemical vapor deposition (PECVD) at 80°C .

Next, we used two targets with different compositions to separately deposit 35-nm-thick ATZO channel layers (referred to sample "S1" and "S2") on the insulator layer under the oxygen partial pressure of 5%. The wt% ratio of SnO_2 and Al_2O_3 in the sample S1 target was 2%:2% and which of S2 was 3%:3%. The SiO_2 and ATZO films were defined pattern by one mask in order to ensure the channel-insulator interface properties. At last, ITO S/D contacts were formed by the same process conditions with gate electrode. It was worth noting that all films were deposited under the room temperature except SiO_2 layer. Besides, the deposition pressure and power of sputtering process were kept to 1.2 Pa and 70W, respectively.

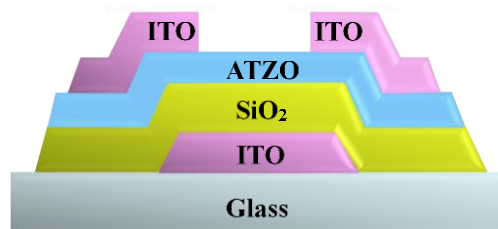


Fig.1 The cross section diagram of ATZO TFT.

The crystal quality of ATZO films was analyzed by X-ray diffraction (XRD, Rigako). The ATZO TFTs were electrical measured by a semiconductor parameter analyzer (Agilent 4156C) at room temperature. The surface morphologies of ATZO films were featured by atomic force microscopy (AFM, SPI3800/SPA400).

3. Results Discussion

The optical transmittance spectra of the two ATZO films is demonstrated in Fig. 2. The result shows the transmittances of both samples are over 80% in the visible light range. The insert in Fig. 2 is the Tauc plots of $(\alpha h\nu)^2$ against photo energy ($h\nu$), which are used to extract optical energy band gap (E_g), where α is the absorption coefficient of the material, E_g value is extracted by the intercept of the linear region extrapolating to $h\nu$ -axis. Compared with sample S1, the E_g of S2 shows blue shift. The result proves that the S2 film with the higher content of dopants has higher carrier concentration, according to the Burstein-Moss effect [8].

Fig. 3 shows the XRD spectra of ATZO films. Since the thicknesses of the films are only 35nm, the intensities of

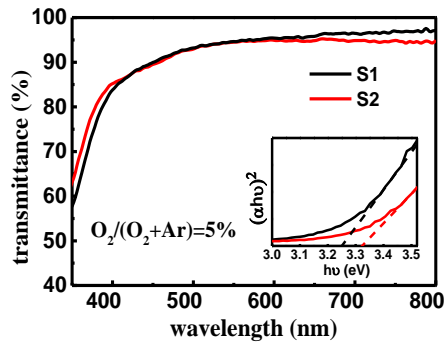


Fig. 2 The optical transmittance spectra of the ATZO Films in the range of 350nm to 800nm. Inset is the Tauc plots of $(\alpha h\nu)^2 - h\nu$.

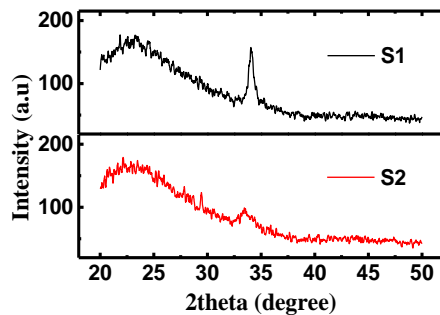


Fig. 3 The XRD spectra of the ATZO films.

the diffraction peaks are weak. Compared with sample S1, the peak of S2 shows broaden FWHM, lower intensity as well as left shift. Indicated from the relatively high content of dopants, the crystal structure of S2 film has extended lattice constant and decreased grain size. However, with much higher density of dopants, the film tends to be amorphous [9]. In conclude, sample S1 with fewer dopants demonstrates better crystal quality.

The transfer curves of the ATZO TFTs were shown in Fig. 4. Both the samples demonstrate excellent characteristics. The sample S2 has a higher I_{on} and a lower V_T than sample S1. The extracted V_T of S1 and S2 are 1.62V and 1.35V, respectively. Since donor (Al^{3+} and Sn^{4+}) densities of sample S2 increase, the carrier concentration improves, which contributes to enhance I_{on} . This result is also consistent with the E_g values (insert in Fig. 2). Besides, it is reported that Sn^{4+} meets the $(n-1)d^{10}ns^0$ ($n \geq 4$) electronic configuration [4], which is useful for improving electrical mobility. With more Sn element in the ATZO film, sample S2 shows better mobility characteristics. The field effect mobility of S1 and S2 are $76.67 \text{ cm}^2/\text{Vs}$ and $102.38 \text{ cm}^2/\text{Vs}$, respectively. In addition, with fewer dopants, sample S2 shows an excellent SS of $155 \text{ mV}/\text{dec}$, which is steeper than S1 ($221 \text{ mV}/\text{dec}$). All the related parameters are specifically

Table I Extracted parameters of ATZO films

No.	I_{on} (mA)	I_{on} / I_{off}	μ_{FE} (cm^2/Vs)	V_T (V)	SS (mV/dec)	E_g (eV)
S1	0.28	1.18×10^7	76.67	1.62	155	3.25
S2	1.03	6.36×10^7	102.38	1.35	221	3.32

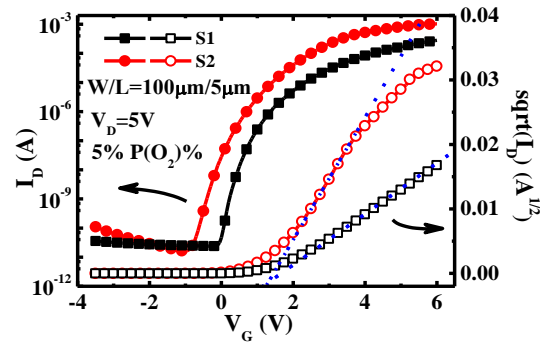


Fig. 4 The transfer characteristics of the two ATZO TFTs. The solid symbols stand for $I_D - V_G$ in the semilog coordinate, the open symbols are $\sqrt{I_D} - V_G$ curves. The blue tangent corresponds to the V_T extraction.

listed in Table I.

The AFM surface morphology images of both samples are demonstrated in Fig. 5. The RMS data of S1 and S2 are 0.55 nm and 0.59 nm , respectively. The S2 shows slightly higher roughness than the S1. Both the films form smooth surfaces.

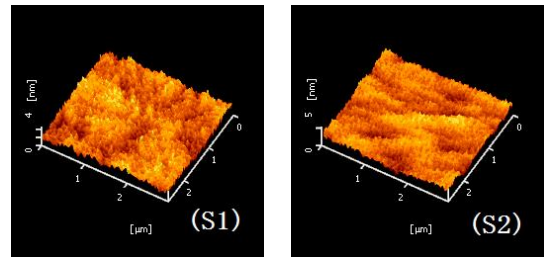


Fig. 5 The AFM morphologies of the ATZO films.

3. Conclusions

The effects of composition on the characteristics of ATZO TFTs are studied. The higher doped sample demonstrates better electrical performance, including a remarkable μ_{FE} of $102.38 \text{ cm}^2/\text{Vs}$ and a higher I_{on} / I_{off} of 6.36×10^7 , which proves the promising applications in display fields.

Acknowledgements

This work is supported by the National Basic Research Program of China (973 program, Grant No. 2011CBA00600) and by the National Natural Science Foundation of China (Grant No. 61275025).

References

- [1] N. Münzrieder, *et al.*, IEEE Trans. Electron Devices, 35 (2014) 69.
- [2] J. Cai, *et al.*, IEEE Trans. Electron Devices, 60 (2013) 2432.
- [3] S. Yang, *et al.*, IEEE Electron Device Lett., 31 (2010) 144.
- [4] H. Hosono, J. Non-Crystalline Solids. 352 (2006) 51.
- [5] K. Nimura, *et al.*, Jpn. J. Appl. Phys. 45 (2006) 4303.
- [6] J. Y. Bak, *et al.*, Ceramics International, 39 (2013) 2561
- [7] Y. Y. Cong, *et al.*, 2014 International Symposia on VLSI Technology, Systems and Applications (2014) 66.
- [8] B. Elias, Phys. Rev. 93 (1954) 632.
- [9] P. Banerjee, *et al.*, J. Appl. Phys., 108 (2010) 043504.